Modelling the Flow of Water in Stratified Layers of Sand

[1]O.I. Popoola, [1]J.A. Adegoke and [2]Alabi, O.O.

[1]Department of Physics, University of Ibadan.
[2]Department of Mathematical and Physical Sciences,
College of Science, Engineering and Technology,
Osun State University, Osogbo.

Abstract

The phenomenon of deflection of flow of water in porous media of different porosities with porosity ratio, ψ , is similar to the fact that there is deviation in fluid flow in a pair of media of different densities. Theoretically, the relationship between preferred direction of flow of water, θ, and the sand layers of porosity ratio, ψ was found to be $\cos\theta = n\psi$ while experimentally it was obtained to be $\cos\theta =1.98\ \ln\psi + 1.13\ (0.5951 \leq \psi \leq 0.9634)$.Thereafter, when the theoretical equation was compared with the experimental result, the value of n ranging from 0 to 1 were found to be appropriate for the theoretical equation to be valid.

Key words: porosity ratio, inlet pipe, outlet pipe, deflection angle.

Introduction:

The greatest danger of groundwater pollution is from surface sources, including sewage sludge, leaking sewers, and polluted water from refuse disposal sites. Wherever any groundwater supply well is constructed, a viable groundwater measure must be taken to prevent contamination by pollutant [14]. One approach is to control the rate of flow (or seepage) or change the direction of the flow of contaminated fluid by using appropriate sand layers of variable porosities [15, 17].

It should be appreciated that soil itself serves as a filter, and its ability to do so depends on its physical attributes such as permeability and porosity [13]. Natural filters have been used as landfill liners to reduce the movement of contaminated fluid from solid waste landfill and waste water disposal into subsurface. [2, 3, 4,6, 7, 12, 13 and 16]. However, a graded filter serves better; it consists of layers of porous materials of different porosities or permeabilities in which the soil particles in a particular layer are coarser than that in the preceding layer [9]. It should be noted that the selection of a good graded filter as a protective layer or a seepage control medium depends on its properties, which can only be determined experimentally. Thus, there is a need for better understanding of the law which governs the flow of fluid through these media which are used as graded filter.

The aim of this work is to model the most preferred direction flow of water across media of different porosities by comparing the theoretical result and experimental result.

The equation obtained earlier by Cedergreen is based on permeability, however, the permeability obtained by Darcy's law for fine-grained sand varies with hydraulic gradient, which makes the law invalid for material within this range. Apart from this, the equation was obtained theoretically and therefore can not be seen as true picture of the real pattern of fluid deflection in non-homogenous medium. Also the range of angle of deflection that can be obtained from the above equation is very small. Thus, there is a need for another parameter which does not vary or change with hydraulic gradient. Porosity was chosen because it does not change with hydraulic gradient for soils or materials of different grain sizes, especially when the grains are of the same size; and it is easily determine in the laboratory [5]. Therefore, we can now determine experimentally the actual relationship between the angle of deflection and the porosities of the media that made up of the heterogeneous medium.

In this research, riverbed sands were used as porous media for the experimental work and their porosities were determined in the laboratory by volumetric approach after necessary processing.

Corresponding author: *Alabi, O.O. : e-mail: geosciencealabi@yahoo.com **Tel:**(+2348035028760)*
.

Theoretical Background

In some instances, a great deal can be learned by studying seepage patterns in cross-sections with soils of more than one permeability vis-à-vis porosities, and such studies have revealed important shortcomings in some commonly accepted beliefs about seepage and drainage [9]

When water flows across a boundary between dissimilar soils, the flow line bend in such a way that light rays are refracted in passing from air into water or from air into glass [9]. The law of conservation of energy forces all natural phenomena to take the line of least resistance. Thus, when water flows from a soil of high permeability into a material of lower permeability, the pattern develops in such a way that the flow remains in the more permeable material for the greatest possible distance. Likewise, if the flow is from a material of low permeability into one of higher permeability, it deflects as soon as possible into the material of higher permeability [9]. To conserve energy, water seeks the easiest paths to travel.

Another way of looking at the behaviour of seepage in sections with more than one permeability is the concept that, other factors being equal, the higher the permeability, the smaller the area required to be passed by a given volume of water. Conversely, the lower the permeability, the greater the area required.

In relation to the amount of energy needed to force water through porous media, the higher th permeability, the lower the energy needed and vice-versa. In seepage, the rate of loss of energy is measured by the steepness of the hydraulic gradient, steep hydraulic gradient should be expected in the zones of low permeability and flat gradients, in zones of high permeability [9].

The way flow lines deflect when they cross the boundaries between soils of different soils of different permeabilities is shown in figure 1. The flow lines bend to confirm the relationship given as

$$\frac{\tan \alpha}{\tan \beta} = \frac{k_2}{k_1} \quad [9] \tag{1}$$

Where

$k_1 = permeability\ of\ medium\ 1$

$k_2 = permeability\ of\ medium\ 2$

$\propto = angle\ between\ the\ flow\ line\ in\ medium\ 1\ and\ the\ boundary$

$\beta\ = angle\ between\ the\ flow\ line\ in\ medium\ 2\ and\ the\ boundary$

Simultaneously, the areas formed by the intersecting line either elongate or shorten, depending on the ratio of the two permeabilities and confirm the relationship given as

$$\frac{c}{d} = \frac{k_2}{k_1} \tag{2}$$

where,

$c = length\ of\ the\ area\ formed\ in\ the\ medium\ 2$

$d = breadth\ of\ the\ area\ formed\ in\ the\ medium\ 2$

In the figure 2a, the second permeability is lower than the first, hence shortened triangles are formed in the second medium. In the figure 2b, the second permeability is greater than the first, so elongated rectangles are formed in the second medium. The deflection relationship is expressed by equation 1 while the equation 2 is extremely useful, as it provides an exact check of the accuracy of flow nets for sections with more than one permeability.

In a similar work carried out by [10] for soil layer of different texture, a similar explanation was given in their results. It was observed that if a finer textured soil layer overlying a coarser-textured layer (Fig. 2a), particularly if the boundary between the two layer is fairly sharp, it will hold more water against drainage than if it is underlain by material of its own texture or a finer textured layer (Fig. 2b and 2c). This is very noticeable if the coarser-textured layer is a sand. It is evident from above the explanations that the volume of water discharged and volume flux can be affected by changes of textures vis-à-vis porosity of the soil profile.

Fig. 3 shows the case when the porosity of soil 2 (ϕ_2) is greater than the porosity of soil 1 (ϕ_1). The flow lines get deflected away from the normal after crossing the interface. The phenomenon of deflection of the flow lines is somewhat similar to refraction of light rays from a dense medium to a sparse medium [1, 8 and 9].

Let α be the angle which the flow line in soil 1 makes with the interface, β be the angle which the flow line in soil 2 makes with the interface and let θ be the angle which the flow line in soil 2 makes with the normal (angle of deflection). Let l_1 and l_2 be the distance travelled by fluid in soil 1 and soil 2 respectively.
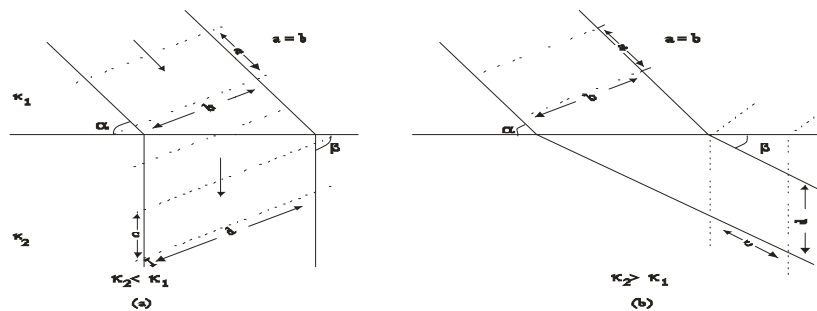
Fig. 1: Transfer conditions at boundaries between soils of different   permeabilities [8, 9]
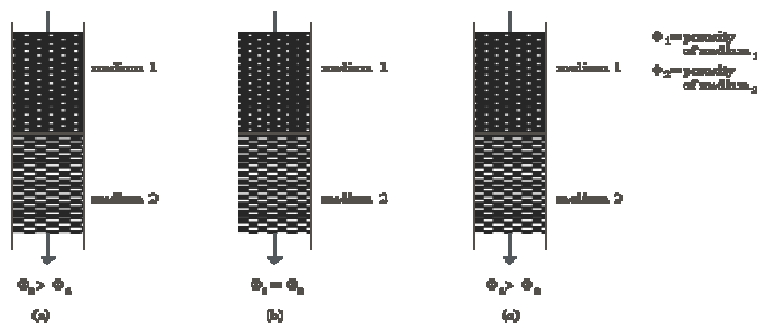

Fig. 2   **Fluid flow in soil layers of different textures** [9, 10]
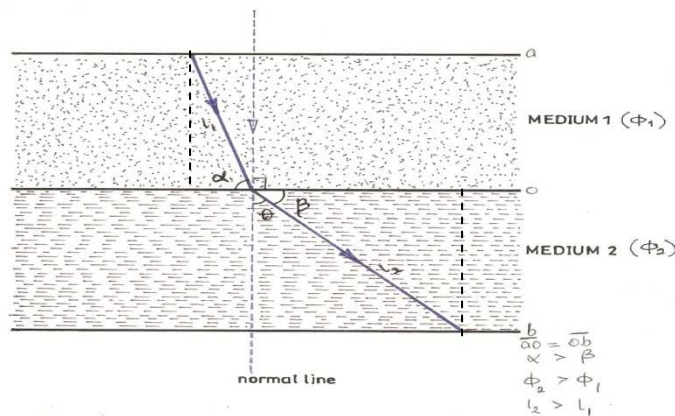
Fig. 3: Fluid flow in non-homogeneous soil mass (Adapted from [9])

By geometry, if $ao = ob$ and $\alpha > \beta$ which implies that $l_2 > l_1$

l_1 = distance travel by fluid in soil1 of porosity ϕ_1

l_2 = distance travel by fluid in soil 2 porosity ϕ_2

α = angle between fluid flow line in soil 1 and the interface

β = angle between fluid flow line in soil 2 and the interface

θ = angle of deflection from the normal in soil 2

From $\Delta b'oc$

$$\sin \alpha = \frac{ob'}{l_1} \qquad\qquad (3)$$

From $\triangle boc$

$$\sin \beta = \frac{ob}{l_2} \tag{4}$$

Equation 1 divided by equation 2 gives

$$\frac{\sin \alpha}{\sin \beta} = \frac{l_2}{l_1}, \qquad (ob = ob') \tag{5}$$

q_1 is the rate of fluid flow per unit time in soil 1 while q_2 is the rate of fluid flow per unit time in soil 2
Thus,

$$q_1 = \frac{l_1}{t} \tag{6}$$

$$q_2 = \frac{l_2}{t} \tag{7}$$

Where
t = travel time, which are equal for fluid to travel in soil 1 and 2.
Equation 6 divided by equation 7 gives

$$\frac{q_1}{q_2} = \frac{l_1}{l_2} \tag{8}$$

This implies that the rate of fluid flow per unit time is proportional to distance travel by fluid.
By using equation 8 in equation 5, we can write

$$\frac{\sin \alpha}{\sin \beta} = \frac{q_2}{q_1} \tag{9}$$

The rate of fluid flow is proportional to porosity, and if the constant of the proportionality is denoted by n, then.

$$\frac{\sin \alpha}{\sin \beta} = n \frac{\phi_2}{\phi_1} \tag{10}$$

For laminar and steady flow in soil 1, angle α will be 90^0. Thus angle α can be assumed to be 90^0. (Fig. 3).
Then equation (8) becomes

$$\frac{1}{\sin \beta} = n \frac{\phi_2}{\phi_1} \tag{11}$$

$$< (\theta + \beta) = 90^0 \qquad \text{(Fig. 3)}$$

Therefore,

$$\beta = 90^0 - \theta \tag{12}$$

By using equation 12 in equation 11, then equation 11 becomes

$$\frac{1}{\sin(90^0 - \theta)} = n \frac{\phi_2}{\phi_1}$$

or

$$\frac{1}{\cos \theta} = n \frac{\phi_2}{\phi_1}$$

which can be written as

$$\cos \theta = n\psi, \qquad (\psi = \phi_1 / \phi_2) \tag{13}$$

Equation 13 shows the relationship between angle of deflection θ and porosity ratio (ψ) of the soils 1 and 2 while *n* is the constant of proportionality. This implies that as porosity of the soil 2 (ϕ_2) increases relatively to porosity of soil 1, porosity ratio (ψ) decreases; and as the porosity ratio decreases the angle of deflection, θ increases. This is true because cosine of angle θ decreases with increasing angle θ.

Equation 13 can therefore be seen as the basis which shows that there is existence of a definite relationship between the

porosities ratio of the soils in which the fluid is flowing through and the angle of deflection; when it flows from one soil to the other. The actual expression shall be determined experimentally.

Methodology

The experimental set-up consisted of a big transparent cylindrical pipe 108.5×10^{-2} m with radius 2.23×10^{-2}m as an inlet pipe and five small equal transparent cylindrical pipe of radius 0.3×10^{-2} m each as outlets (Fig. 4). Each of the outlet pipes was joined to the centre of the circular plastic plate on the top of the inlet pipe at different angles θ of 0^0, 20^0, 50^0, 70^0 and 90^0 from normal point or line. Water was allowed to flow through the empty inlet pipe into outlet pipes for a period of 60seconds and this serves as a control experiment. The discharge volume of water at each outlet was collected with beaker and measured with measuring cylinder. This was done at different tilting or inclination angle α of 0^0, 5^0, 10^0, 15°, and 20^0. Thereafter, the inlet pipe and outlet pipes were filled with the same sample at a time and the volume of water discharged through each outlet pipe was measured for different angle of inclination α. This was repeated for all the samples. Then, all the five outlets were filled with the sample of higher porosity relatively to that the inlet pipe to constitute layered heterogeneous media. The volume of water discharged from each outlet was measured. This was also done at different angle of inclination α in order to know the effect of angle of inclination on fluid flow rate for each sample and cross-section of samples. The sample in the inlet pipe was later changed in turn in order to obtain different porosities ratios and the volume of water discharged from the outlets in different cases were measured directly with measuring cylinder. The volume flux q(m^{-1}) or specific discharge was then computed from the volumetric flow rate Q(m^{3}s^{-1}) by dividing it with the cross-sectional area, 2.83×10^{-5}m^2 of the outlet pipe. Fig. 5 is the schematic diagram of fig. 4 to show the experimental set up clearly.
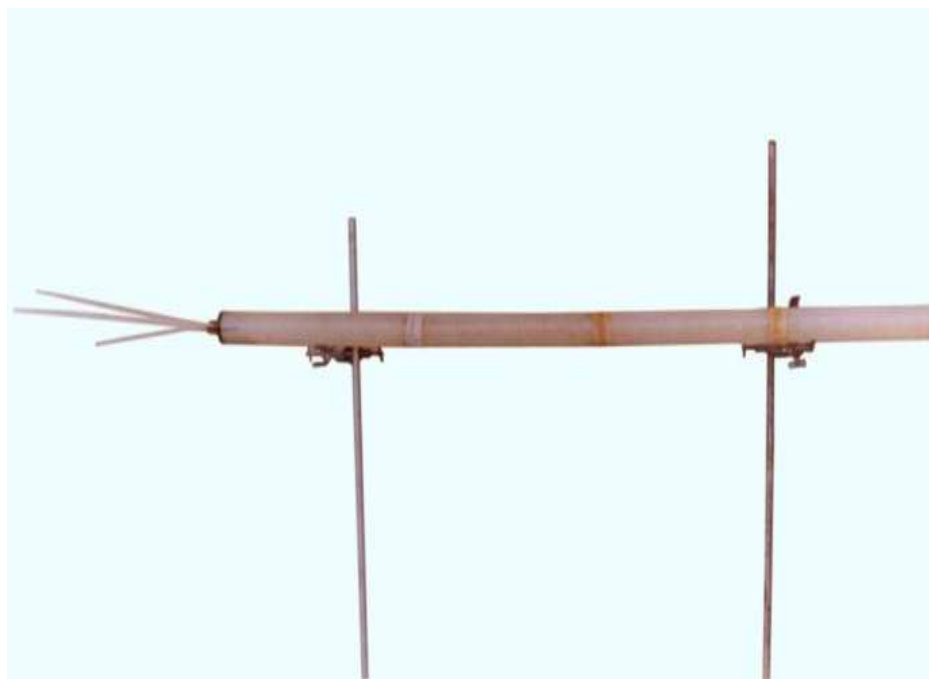

Fig. 4: Experimental setup for determination of volume
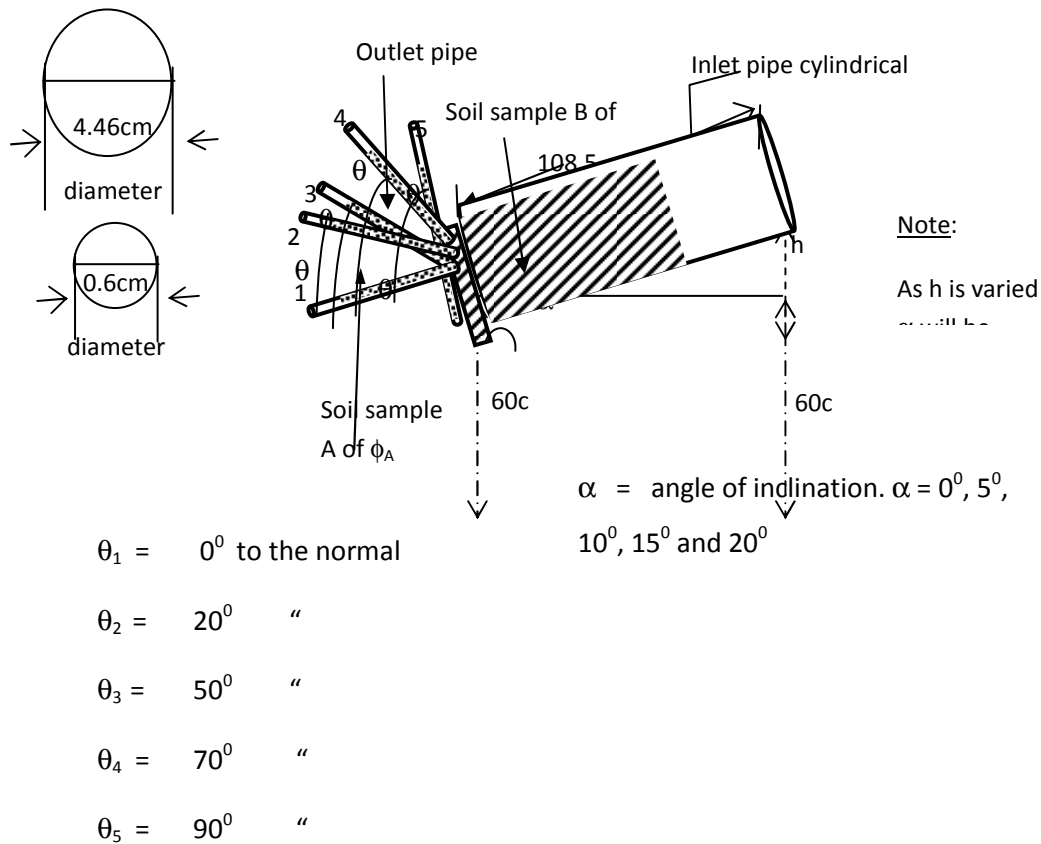flux at different outlet angles

Outlet pipe

Inlet pipe cylindrical

4.46cm diameter

0.6cm diameter

Soil sample B of

108.5

Note:

As h is varied

Soil sample A of ϕ_A

60c 60c

α = angle of inclination. $\alpha = 0^0, 5^0, 10^0, 15^0$ and 20^0

θ_1 = 0^0 to the normal

θ_2 = 20^0 "

θ_3 = 50^0 "

θ_4 = 70^0 "

θ_5 = 90^0 "

Fig. 5: Schematic diagram of experimental set up to determine volume flux at different angles of inclination

Results and Discussion

Table 1 presents the value of water discharge, *V,* from each outlet pipes at various angles of inclination of the second experimental setup; when both the inlet and outlet pipes were free of porous material. This serves as a control experiment to verify if the setup is in order. These values were obtained in a very direct way, by collecting the values of water discharged for 60seconds from each outlet simultaneously. Thereafter, the volumetric flow rate and volume flux for this control experiment were determined and presented in Table 2 and 3 respectively.

The volume flux of water discharged through each outlet for different porosity ratios were determined and presented in Tables 4 – 13 for porosity ratios 0.5952, 0.6250, 0.6868, 0.7508, 0.7929, 0.8325, 0.8667, 0.9100, 0.9148 and 0.9523 respectively.

Table 14 is an extract from the values of volume flux presented in Tables 4 – 13. This was done in order to show at a glance, outlet angles with maximum volume flux with respect to each porosity ratios, which indicates the angle of deflection (or preferred direction of flow) of water through that media. In addition, this will be of help in establishing the relationship that exist between the porosity ratio and angle of deflection.

In order to establish the relationship between preferred direction of flow and the porosity ratio, angle of deflection was plotted against porosity ratio. This relationship was establish by curve fitting (Fig. 6) with correlation coefficient of 0.97.

The results from the control experiment of the setup shows that the volume flux, *q* for outlet pipes of different angles at a given angle of inclination are more less equal (Table 3). This implies that irrespective of the angle of outlet, when water flows through empty inlet and outlets pipes, the volume flux will be the same. Thus, there would not be deflection of fluid when there are no material medium in the inlet and outlet pipes. Also, this indicates that there is perfectness in the model or setup for the work. However, it was noted that volume flux increases with increasing angle of inclination. This is in order, because angle of inclination can be likened to hydraulic gradient in Darcy's law.

When the pipes were filled with sand, the volume flux follow similar pattern but there was uniform fractional decrement in

volume flux as compared to when the sand were absent. This is so because the presence of the material medium (sand sample) serves as 'impedance' for free flow of fluid. Thus, like control experiment, there was no indication of any deflection when the porosity of the media in both inlet and outlet pipes are the same.

The ratio of the porosity of the sample in the inlet to that of sample in outlet pipes is called porosity ratio. The results from ten sets of porosity ratios considered show that volume flux are not the same in all the outlet pipes (Tables 4 – 13). These results are contrary to that of the control experiments and when the porosities of sample in inlet pipe and outlet pipes are the same. It was observed that there is a definite pattern for outlet angle that produces highest volume flux with respect to porosity ratio, which indicates the direction of deflection of water in the second medium with respect to porosity ratio of the two media.

It is clearly shown that the outlet angle with the highest volume flux varies for different porosity ratios. For the least porosity ratio (0.5952), the outlet of angle 90^0 produces highest volume flux while highest volume flux was obtained for highest porosity ratio (0.9523) at outlet of angle 0^0 (Table 14). This implies that the angle of deflection, θ of the water decreases as porosity ratio increases. This can also be stated in this form that, as the porosity of the medium the water flows into is increasing, the lower the porosity ratio and the greater the deflection angle, θ in that medium. If the porosity ratio decreases, it is similar to the fact that densities of a pair of media very sharply and it is expected that deviation should be more. This result corroborates with earlier results obtained by [9, 10] which showed that when fluid low from a material of flow permeability into one of higher permeability, it deflects as soon as possible into material of higher permeability [9, 10].

In order to establish the relationship between deflection angle θ of the fluid flow and the porosity ratio, the cosine of angle θ was computed and plotted against porosity ratio. The equation of the graph was given to be $\cos\theta = 1.98\ln(\psi) + 1.13$ by curve fitting. From this equation, the maximum angle of deflection in stratified porous medium made up of fine and medium sand will be 89.4^0. this is true because the maximum value of the porosity ratios will be 0.5682 (0.25/0.44) for sands categorized under fine and medium sands (Freeze and Cherry, 1979).

Also, this equation implies that for a range of porosity ratios 0.5651 to 0.9364, the deflection angle 0^0 to 90.0^0 can be obtained.

Considering the effect of the angle of inclination on the deflection of water at various porosity ratios, it was observed that angle of inclination does not have a significant effect on the deflection angle, θ for angles of inclination, α ranges from 0^0 to 20.0^0 used in this work. However the volume flux vis-a-vis seepage velocity increases as angle of inclination increases for all porosity ratios.

Equation 13 was proposed as the equation that shows the relationship between angle of deflection, θ and porosity ratio, ψ. However there is a need to determine the value and nature of n in the theoretical equation. The theoretical equation and experiment equation were compared by equating them to each other, the result obtained shows that n is not constant, but ranges from 0 to 1, and its value is dependent of porosity ratio, ψ. The essence of seeking for the value of n is to validate the experiment result and to widen the range of deflection, θ for angles that could not be accommodated by the experimental set up.

The experiment equation Cos θ = 1.98 In ψ + 1.13 indicates that angle of deflection (or preferred direction of flow) with angle θ depends on the porosity ratio ψ. It is interesting to note that as porosity ratio decreases (i.e. the greater the difference between the porosities of the media) the greater the angle, θ just as for theoretical expression (eqn. 13).

Table 1: Values of volume of water discharge V x 10^{-6} (m^3) when both inlet and outlet pipes were without porous medium

Angle of Inclination, α	Outlet angle θ				
	0°	20°	50°	70°	90°
0°	0	0	0	0	0
5°	22.27 ± 0.06	22.21 ± 0.07	21.95 ± 0.06	22.50 ± 0.12	22.30 ± 0.09
10°	26.40 ± 0.03	26.47 ± 0.12	26.13 ± 0.12	26.20 ± 0.12	26.07 ± 0.06
15°	38.20 ± 0.12	38.33 ± 0.15	38.07 ± 0.06	37.90 ± 0.17	38.09 ± 0.15
20°	52.54 ± 0.19	52.00 ± 0.12	52.40 ± 0.19	52.13 ± 0.06	52.52 ± 0.04

Table 2: Values of volumetric flow rate Q x 10^{-8} (m^3/s) when both inlet and outlet pipes were without porous medium

Angle of inclination, α	Outlet angle, θ				
	0°	20°	50°	70°	90°
0°	0	0	0	0	0
5°	37.12 ± 0.06	37.02 ± 0.07	36.58 ± 0.06	37.50 ± 0.12	27.17 ± 0.09
10°	44.00 ± 0.03	44.12 ± 0.12	43.55 ± 0.12	43.67 ± 0.12	43.45 ± 0.06
15°	63.67 ± 0.12	63.88 ± 0.15	63.45 ± 0.06	63.17 ± 0.17	63.48 ± 0.15
20°	87.57 ± 0.19	86.67 ± 0.12	87.33 ± 0.19	86.88 ± 0.06	87.53 ± 0.04

Table 3: Values of volume flux q x 10^{-3} (ms^{-1}) when both inlet and outlet pipes were without porous medium

Angle of Inclination, α	Outlet angle, θ				
	0°	20°	50°	70°	90°
0°	0	0	0	0	0
5°	13.12 ± 0.06	13.08 ± 0.07	12.93 ± 0.06	13.25 ± 0.12	13.13 ± 0.09
10°	15.55 ± 0.03	15.59 ± 0.12	15.39 ± 0.12	15.43 ± 0.12	15.35 ± 0.06
15°	22.50 ± 0.12	22.57 ± 0.15	22.42 ± 0.06	22.32 ± 0.17	22.43 ± 0.15
20°	30.94 ± 0.19	30.63 ± 0.12	30.86 ± 0.19	30.70 ± 0.06	30.93 ± 0.04

Table 4: Values of volume flux q x 10^{-3} (ms^{-1}) for porosity ratio 0.5952   (ϕ_A/ϕ_E)

Angle of inclination, α	Outlet angle, θ				
	0°	20°	50°	70°	90°
0°	0	0	0	0	0
5°	0.43 ± 0.03	0.92 ± 0.06	1.08 ± 0.03	1.06 ± 0.06	1.30 ± 0.03
10°	1.02 ± 0.07	1.02 ± 0.07	2.59 ± 0.03	2.78 ± 0.03	3.42 ± 0.06
15°	1.10 ± 0.09	2.11 ± 0.06	3.85 ± 0.03	4.52 ± 0.06	5.11 ± 0.12
20°	1.46 ± 0.07	2.48 ± 0.12	4.01 ± 0.06	5.47 ± 0.03	6.27 ± 0.09

Table 5: Values of volume flux q x 10^{-3} (ms^{-1}) for porosity ratio 0.6250 (ϕ_A/ϕ_D)

Angle of Inclination α /degree	Outlet angle, θ				
	0° q x 10^{-3} (ms^{-1})	20° q x 10^{-3} (ms^{-1})	50° q x 10^{-3} (ms^{-1})	70° q x 10^{-3} (ms^{-1})	90° q x 10^{-3} (ms^{-1})
0°	0	0	0	0	0
5°	0.24 ± 0.06	0.87 ± 0.09	1.26 ± 0.03	1.06 ± 0.09	0.35 ± 0.03
10°	0.35 ± 0.06	1.61 ± 0.06	1.30 ± 0.03	3.14 ± 0.12	0.49 ± 0.03
15°	0.71 ± 0.03	2.16 ± 0.07	3.14 ± 0.06	4.64 ± 0.12	0.71 ± 0.03
20°	0.75 ± 0.06	2.52 ± 0.06	4.83 ± 0.06	5.95 ± 0.06	1.43 ± 0.03

Table 6: Values of volume flux q x 10⁻³ (ms⁻¹) for porosity ratio 0.6868 (ϕ_A/ϕ_C)

Angle of Inclination, α	Outlet angle, θ				
	0°	20°	50°	70°	90°
0°	0	0	0	0	0
5°	0	0.59 ± 0.00	0.73 ± 0.03	0.98 ± 0.06	0.25 ± 0.06
10°	0.13 ± 0.07	1.02 ± 0.03	0.96 ± 0.00	2.71 ± 0.12	0.35 ± 0.06
15°	0.15 ± 0.03	1.26 ± 0.06	1.18 ± 0.03	4.48 ± 0.09	0.75 ± 0.03
20°	1.70 ± 0.03	1.65 ± 0.06	6.22 ± 0.06	4.60 ± 0.03	1.30 ± 0.03

Table 7: Values of volume flux q x 10⁻³ (ms⁻¹) for porosity ratio 0.7508 (ϕ_A/ϕ_B)

Angle of Inclination, α	Outlet angle, θ				
	0°	20°	50°	70°	90°
0°	0	0	0	0	0
5°	0.13 ± 0.03	0.71 ± 0.07	0.74 ± 0.03	0.63 ± 0.06	0.12 ± 0.03
10°	0.24 ± 0.03	0.75 ± 0.03	0.82 ± 0.03	0.75 ± 0.09	0.20 ± 0.03
15°	0.61 ± 0.06	0.75 ± 0.09	2.24 ± 0.05	1.46 ± 0.06	0.43 ± 0.09
20°	0.62 ± 0.06	0.82 ± 0.03	4.91 ± 0.03	3.14 ± 0.03	0.75 ± 0.03

Table 8: Values of volume flux q x 10⁻³ (ms⁻¹) for porosity ratio 0.7929 (ϕ_A/ϕ_C)

Angle of Inclination, α	Outlet angle, θ				
	0°	20°	50°	70°	90°
0°	0	0	0	0	0
5°	0	0.16 ± 0.03	4.36 ± 0.06	1.85 ± 0.09	0.90 ± 0.03
10°	0.12 ± 0.03	1.85 ± 0.03	5.11 ± 0.06	3.93 ± 0.06	2.43 ± 0.03
15°	1.26 ± 0.03	2.71 ± 0.06	6.11 ± 0.17	5.13 ± 0.03	3.40 ± 0.09
20°	2.64 ± 0.06	3.41 ± 0.03	11.98 ± 0.12	10.96 ± 0.06	5.70 ± 0.12

Table 9: Values of volume flux q x 10⁻³ (ms⁻¹) for porosity ratio 0.8325 (ϕ_B/ϕ_D)

Angle of inclination, α	Outlet angle θ /degree				
	0°	20°	50°	70°	90°
0°	0	0	0	0	0
5°	0	0	4.01 ± 0.06	1.61 ± 0.03	0.43 ± 0.03
10°	0	0	4.95 ± 0.06	3.73 ± 0.06	1.85 ± 0.06
15°	0.90 ± 0.03	1.02 ± 0.03	5.07 ± 0.12	4.91 ± 0.06	3.65 ± 0.03
20°	1.26 ± 0.03	2.59 ± 0.06	11.43 ± 0.15	10.96 ± 0.06	4.56 ± 0.09

Table 10: Values of volume flux q x 10^{-3} (ms^{-1}) for porosity ratio 0.8667 (ϕ_C/ϕ_E)

Angle of inclination, α	Outlet angle, θ				
	0°	20°	50°	70°	90°
0°	0	0	0	0	0
5°	0	6.13 ± 0.06	1.89 ± 0.03	0.90 ± 0.06	0.61 ± 0.03
10°	0.16 ± 0.06	9.10 ± 0.03	4.56 ± 0.03	2.71 ± 0.06	2.04 ± 0.03
15°	1.34 ± 0.06	12.45 ± 0.09	7.35 ± 0.06	6.09 ± 0.09	5.35 ± 0.07
20°	3.07 ± 0.03	15.52 ± 0.07	12.65 ± 0.03	7.33 ± 0.12	6.09 ± 0.06

Table 11: Values of volume flux q x 10^{-3} (ms^{-1}) for porosity ratio 0.9100 (ϕ_C/ϕ_D)

Angle of inclination, α	Outlet angle, θ				
	0°	20°	50°	70°	90°
0°	0	0	0	0	0
5°	0.20 ± 0.07	2.71 ± 0.03	1.85 ± 0.03	1.43 ± 0.07	0
10°	2.43 ± 0.06	5.07 ± 0.03	3.14 ± 0.06	1.46 ± 0.03	0.12 ± 0.03
15°	6.11 ± 0.09	8.40 ± 0.06	4.29 ± 0.06	2.64 ± 0.06	1.02 ± 0.03
20°	7.19 ± 0.06	8.67 ± 0.03	4.36 ± 0.12	3.92 ± 0.03	1.61 ± 0.03

Table 12: Values of volume flux q x 10^{-3} (ms^{-1}) for porosity ratio 0.9148 (ϕ_B/ϕ_C)

Angle of inclination, α	Outlet angle, θ				
	0°	20°	50°	70°	90°
0°	0	0	0	0	0
5°	2.48 ± 0.09	0.90 ± 0.06	0.90 ± 0.03	0.75 ± 0.03	0
10°	5.13 ± 0.06	1.89 ± 0.06	2.43 ± 0.03	1.89 ± 0.03	0
15°	8.31 ± 0.03	2.71 ± 0.03	2.64 ± 0.06	2.43 ± 0.03	0.12 ± 0.03
20°	8.41 ± 0.06	7.35 ± 0.03	5.11 ± 0.03	4.29 ± 0.06	0.12 ± 0.00

Table 13: Values of volume flux q x 10^{-3} (ms^{-1}) for porosity ratio 0.9523 (ϕ_D/ϕ_E)

Angle of Inclination, α	Outlet angle, θ				
	0°	20°	50°	70°	90°
0°	0	0	0	0	0
5°	7.88 ± 0.09	2.43 ± 0.06	1.26 ± 0.03	0	0
10°	11.02 ± 0.06	5.35 ± 0.06	4.29 ± 0.06	0.20 ± 0.06	0
15°	16.82 ± 0.03	8.41 ± 0.03	7.19 ± 0.06	2.48 ± 0.12	0.12 ± 0.03
20°	17.80 ± 0.12	8.57 ± 0.12	8.31 ± 0.09	6.01 ± 0.07	0.16 ± 0.03

Table 14: Values of porosities ratio, angle of deflection and cosine of angle of deflection

Porosity ratio	Angle of Deflection	Cosθ
0.9523	0	1
0.9148	0	1
0.9100	20	0.9397
0.8667	20	0.9397
0.8325	50	0.6428
0.7929	50	0.6428
0.7508	50	0.6428
0.6868	70	0.3420
0.6250	70	0.3420
0.5952	90	0

$$\cos\theta = 1.98\ln(\psi) + 1.13$$

$$(R^2 = 0.97)$$

Porosity Ratio
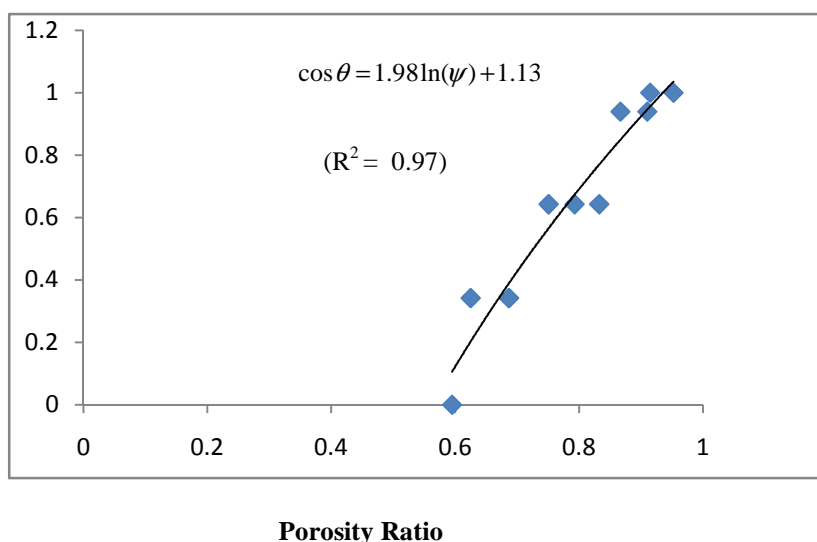
Fig. 6: Plot of Cosθ against porosity ratio ψ

Conclusion

If water flows through layers of sand of different porosities with porosity ratio, ψ, the relationship between the preferred direction of flow at angle, θ in the second layer was found to be *cos θ = 1.98ln(ψ) + 1.13,* for porosity ratios within 0.5651 to 0.9364. The preferred direction of flow of angle 89.4^0 was obtained when water flows from fine grained sand of minimum porosity 0.25 to medium grained sand of maximum porosity 0.44 .The was obtained for sands categorized under fine and medium grained because the porosity ratio for this media is 0.5682(0.25/0.44).

This model could be useful in the process whereby the contaminated fluid is to be directed to unwanted portion of land rather than reducing the seepage. When a material or sand of lower porosity or permeability is used as protective layer, it is possible for the soil or surrounding to be contaminated due to low seepage. The alternative option is to deflect the contaminated water from the source of water. If there is a need for this, porous materials of appropriate porosities can arranged in layers to design a stratified protective layer to deflect the contaminated fluid to a specified directions. Also, the model could be useful for selective irrigation, whereby different crops requiring different quantities of water can be irrigated from a single source of water supply. This can be done by selecting appropriate sands of known porosities to constitute a layered medium for deflecting the incident water at different angles from the original direction.

References

[1]   Arora, K. R. 2009. Soil mechanics and foundation Engineering. (Geotechnical 7th Engineering) Edition. Standard publishers distributors, Delhi.

[2]   Benson, C.H. and Daniel, D.E. 1990. Influence of clods on the hydraulic conductivity of compacted clay. *Journal of Geotechnical Engineering, ASCE* . 120(8):129 – 152.

[3]   Benson, C.H. and Trast, J. 1995. Hydraulic conductivity of thirteen compacted clays. *Clay and clay minerals* 43(6):669.

[4]   Benson, C.H. Zhai, and Wang, X. 1994. Estimating hydraulic conductivity of compacted clay lines. *Journal of Geotechnical Engineering, ASCE*. 120(2): 366-387

[5]   Bell, F.G.2007. Engineering Geology. 2nd Edition, Butterworth-Heinemann, Elsevier print, Burlington, USA.

[6]   Boadu, F. K. 2000. Hydraulic conductivity of soils from grain size distribution: New models. *Journal of Geotechnical and Geoenvironmental Engineering, ASCE* 126(8): 739- 746.

[7]   Boynton, S. S. and Daniel, D.E. 1985. Hydraulic conductivity tests on compacted clay, *Journal of Geotechnical Engineering, ASCE.* 3(4): 465 – 478

[8]   Casagrande, A., 1937. Seepage through dams. Harvard university publication 209. Reprinted from *Journal of the New England water Association*

[9]   Cedergreen, H.R, 1976. Drainage and flow nets. Willey- Interscience Publication, New York.

[10]   Eagleman, J.R. and Jamison, V.C. 1962. Proceeding of America Soil Science society. 519.

[11]   Freeze, R.A. and Cherry J.A. 1979. Groundwater. Prentice- Hall, Inc. Englewood cliffs, NJ. 404.

[12]   Foreman, D.E. and Daniel, D.E. 1986. Permeation of compacted clay with organic chemicals. *Journal of Geotechnical Engineering, ASC*E, 1112(7): 30-31.

[13]   Henry, D. F. 2003. Fundamentals of soil science. 8th Edition. John wiley and sons, New York. 95- 99.

[14]   Hiscock, K. M., Loveit, A.A., Brainard, J. S. and Parfilt, J. P. 1995. Groundwater vulnerability assessment: two case studies using GIS Methodology *Quarterly Journal Engineering Geology,* 28: 179-194

[15]   Leonards, G.A. 1962. Foundation engineering. Mc Graw-Hill, New York. 107- 139.

[16]   Rowel, R. K. Quigley, R.M and Booker, J.R. 1995. Clay barrier system for waste disposal facilities. Chapman and Halpl, London. 390

[17]   Silliman, S.E., Zheng, L. and Conwell, P. 1998. The use of laboratory experiments for the study of conservative solute transport in heterogeneous porous media. *Hydrogeology Journal*, U.S. 6: 166-177